Hindawi
Journal of Chemistry
Volume 2019, Article ID 1907083, 9 pages
https://doi.org/10.1155/2019/1907083

Research Article

Decomposition of *Bis*(N-benzyl-salicydenaminato)zinc (II) Complex for the Synthesis of ZnO Nanoparticles to Fabricate ZnO-Chitosan Nanocomposite for the Removal of Iron (II) Ions from Wastewater

Thokozani Xaba, Patli Phillia Mongwai, and Mahadi Lesaoana

Department of Chemistry, Vaal University of Technology, P/Bag X021, Vanderbijlpark, South Africa

Correspondence should be addressed to Thokozani Xaba; thokozanix@vut.ac.za

Received 2 August 2018; Revised 19 November 2018; Accepted 27 November 2018; Published 2 January 2019

Academic Editor: Carlos A. Martínez-Huitle

The whole world is faced with a huge challenge of the shortage of clean water due to industrialization and the intimidation of climate change. Poor water quality distresses many areas of human's well-being. Although there are existing technologies for water treatments, many of these methods utilize toxic substances which create more problems into the environment. The preparation of *bis*(N-benzyl-salicydenaminato)zinc (II) complex and the synthesis of zinc oxide nanoparticles via the thermal decomposition of zinc complex together with the fabrication of ZnO-chitosan nanocomposites for the removal of iron (II) ions from wastewater is reported. The optical properties of the synthesized nanoparticles showed band edges that are red-shifted in wavelengths when the decomposition temperature was increased. The XRD patterns displayed the hexagonal ZnO phase for the synthesized nanoparticles. TEM images revealed spherical-shaped particles which became agglomerated when the temperature was increased. The parameters such as pH, contact time, and initial concentration were investigated during the water treatment. The pH = 6 was found to be optimum, and the highest percentage removal was recovered after three hours for both adsorbents.

1. Introduction

The high level of metals in our aqueous systems may cause major problems to the environment, humans, and animal lives [1]. The increase of the utilization of the heavy metals in the industry sectors has resulted in the increase of metallic substances in natural water sectors [2]. The existence of these metal ions such as iron is perhaps the most common water difficulty that is faced by water authorities. Generally, iron occurs in two oxidation states, reduced divalent ferrous (Fe(II)) and oxidized trivalent ferric (Fe(III)) [3]. The removal of toxic heavy metals such as iron from the environment and wastewater systems has become an important challenge in our days. The removal process should be simple, operative, and of low cost. Numerous methods have been used to remove Fe(II) ions from wastewater which include complexation, adsorption, bioremediation, biosorption, ion exchange, chemical precipitation, cementation, coagulation and flocculation, and membrane processes [4]. However, adsorption has turned out to be one of the alternative treatment techniques for the removal of heavy metals recently since it is promoting the applications of low-cost adsorbents [5].

ZnO is a conventional wide band-gap semiconductor which is environmental friendly and compatible with living organisms. ZnO is also regarded as nontoxic and harmonious with the human skin by forming a suitable preservative for fabrics and surfaces which are associated with skin [6]. These materials can be used in numerous fields such as UV light-emitting devices [7], photocatalysts [8], hydrothermal process [9], cosmetic industries [10], and pharmaceuticals. Several methods have been reported for the synthesis of zinc oxide nanomaterials which include precipitation [11], sol-gel [12], wet chemical synthetic method

[13], etc. Nanomaterials have shown great potential for their applications in wastewater treatment. ZnO materials are capable of operating in water treatment via various nanotechnology routes [14]. El Saeed and his colleagues synthesized ZnO through direct precipitation technique using $Zn(NO_3)_2{\cdot}6H_2O$ and $(NH_4)_2CO_3$ at 40°C. The precursor was calcinated for 2 hr at 550°C. The TEM images showed the nonagglomerated ZnO nanoparticles with an average particle size of 20 nm [15]. Kumar et al. reported the synthesis and the use of low band-gap ZnO nanoparticles for water treatment, recently [16]. The preparation of zinc oxide nanoparticles for water disinfection was reported by Dimapilis and coworkers. They discovered that ZnO can be very effective in various strains of microorganisms [17]. The preparation of zinc oxide from modified chitosan and its morphological studies was reported by Thirumavalavan et al. [18]. They observed that the surface-modified chitosan was showing enhanced surface properties. There are many other researchers who have developed numerous methods for synthesizing zinc oxide nanomaterials, but the disadvantage of these techniques is that of the usage of toxic and expensive starting materials to prepare these nanoparticles. Iron as a heavy metal in wastewater can be removed by different methods such as electrocoagulation [19–21].

The objective of this study was to stress out the substantial application of low-cost materials for the water treatment process. Recently, salicylaldehyde has been used to prepare several substances due to its low cost to form inexpensive materials for biological processes. The preparation of zinc complex from reaction of salicylaldehyde, amine, and metal salt is reported. The metal complex was used to produce ZnO nanoparticles through the thermal decomposition technique which is a simple and very cheap method that produces nanomaterials which are friendly to the environment. These nanoparticles were then incorporated with chitosan which is a natural biopolymer material to form ZnO-chitosan nanocomposites. The nanocomposites were utilized in the treatment of wastewater to remove Fe(II) ions. The percentage removal of iron (II) ions from water was explored using pure chitosan solution and ZnO-chitosan nanocomposites. The effect of pH, contact time, and initial metal ion concentration was investigated.

2. Experimental

2.1. Materials. Zinc acetate dihydrate, salicylaldehyde, benzamine, methanol, acetone, toluene, chitosan, and ferrous ammonium sulfate hexahydrate. All the chemical substances and reagents used in this study were of analytical grade and were utilized without any further purification.

2.2. Preparation of the Zinc Complex [$C_{26}H_{20}N_2O_2Zn$]. The complex was produced using the reported procedure [22]. Briefly, an equimolar of benzamine (10 mmol) was added into salicylaldehyde (10 mmol) in methanol followed by the addition of zinc (II) acetate (5 mmol) in methanol into a 100 mL two-necked flask. The mixture was refluxed at a temperature of 50°C for 3 hrs. The formed precipitate was then filtered, washed three times with acetone, and dried in a desiccator. *The product was obtained as a* light yellow solid, *m.pt. 178°C, CHNO analysis: Calc.: C, 68.20; H, 7.94; N, 6.19; O, 6.99. Found: C, 68.12; H, 7.28; N, 5.77; O, 6.79. Significant FTIR bands: v(C=N): 1585 cm^{-1}, v(C-O): 1405 cm^{-1}, v(Zn-O): 511 cm^{-1}, v(Zn-N): 462 cm^{-1}.*

2.3. Synthesis of Zinc Oxide Nanoparticles. A sample of the dry zinc precursor (0.5 g) was added into a 5 mL cleaned and dried ceramic boat. The boat was then transferred inside a combustion tube which was then transported into the tube furnace under the fume hood. The sample was calcinated at a temperature of 300°C under the inert environment for an hour. The product was allowed to cool down to room temperature in the furnace. The method was repeated at 400 and 500°C to investigate the effect of temperature. The resulting zinc oxide nanoparticles were dispersed in toluene for further analysis.

2.4. Preparation of ZnO-Chitosan Nanocomposites. The synthesized ZnO nanoparticles (~3 mg) were dispersed in 10 mL of distilled water. The filtered solution was then transferred into a beaker with 0.5% chitosan (50 mL) solution. The mixture was enclosed with a foil and ultrasonicated for 3 hr to ensure complete combination. The prepared ZnO-chitosan nanocomposite solutions were then further utilized in water treatment.

2.5. Batch Adsorption Experiments. A solution of heavy metal (1000 ppm) of ferrous ammonium sulfate was prepared and used as a stock solution. Different concentrations of this solution ranging from 1 to 50 ppm were prepared and used for adsorption studies at room temperature to investigate optimum conditions such as the effect of pH, concentration, and contact time in a 100 mL beaker. ZnO-chitosan nanocomposites or 0.5% chitosan (5,00 mL) solution was added into the stock solution. The pH of the solution was audited to the anticipated values by adding 0.1 M NaOH or 0.1 M HCl.

2.6. Characterization

2.6.1. Fourier Transform Infrared (FTIR) Spectroscopy (FTIR). The FTIR analysis of zinc complex was conducted at room temperature in a scan range between 400 and 4000 cm^{-1} from a Bruker FTIR tensor 27 spectrophotometer.

2.6.2. Elemental Analyzer (EA). Microanalysis was accomplished on a PerkinElmer automated model 2400 series II CHNS/O analyzer.

2.6.3. Thermogravimetric Analysis (TGA). A PerkinElmer Pyris 6 TGA that was conducted at 20°C min^{-1} heating rate from 30 to 900°C in a closed perforated aluminium pan under nitrogen gas was utilized for thermal analysis.

2.6.4. UV-Visible Spectroscopy (UV-Vis) and Photoluminescence (PL). The absorption and emission spectra of ZnO nanoparticles were obtained using UV-1800 Shimadzu spectrophotometer and Gilden Fluorescence.

2.6.5. X-Ray Diffraction (XRD). Philips X'Pert diffractometer that applies secondary monochromated Cu Kα radiation (λ = 1.54060 A) at 40 kV/30 mA was used to collect XRD patterns.

2.6.6. Transmission Electron Microscopy (TEM). Transmission electron microscopy (TEM) images were collected from a Tecnai F30 FEG TEM instrument at an accelerating voltage of 300 kV.

2.6.7. Atomic Adsorption Spectroscopy (AAs). AAs analysis was accomplished on the AA-7000 Shimadzu model coated GFA-7000 graphite furnace atomizer.

3. Results and Discussion

The chemical reaction between salicylaldehyde, amine, and zinc acetate in methanol at a temperature of 50°C produced *bis*(N-benzyl-salicydenaminato)zinc (II) complex as shown in Scheme 1. The precursor was then used to synthesize zinc oxide nanoparticles by thermal decomposition. The incorporation of ZnO nanoparticles into chitosan to form polymer nanocomposites was explored. The nanocomposite and chitosan were then used in water treatment.

3.1. Structural Analysis. Figure 1 displays the FTIR spectrum of *bis*(N-benzyl-salicydenaminato)zinc(II) complex that shows a strong band at 1590 cm^{-1} which is due to ν(C=N) of the imine. The strong bands were also detected at 1180–1405 cm^{-1} which are due to the phenolic ν(C–O) stretching. The stretching frequencies that confirm the coordination of nitrogen and oxygen atom into metal ion were also detected and allocated at 510 and 450 cm^{-1} which are attributed to the Zn–O and Zn–N bonds. These outcomes were similar to the reported results [23].

The thermal decomposition profile of *bis*(N-benzyl-salicydenaminato)zinc (II) complex was investigated using the thermogravimetric analysis linked with differential thermogravimetric analysis (TGA/DTA) (Figure 2). The TGA shows that the prepared zinc complex is stable up to 241°C and shows a single-stage decomposition arrangement which is shown as a dotted line in the DTA graph. This weight loss of 63% in the single-stage decomposition is in the range of 241–407°C, which can be attributed to the loss of the ligand moiety with its oxidative degradation to metal oxide, beyond 407°C. This is due to high degree of electron delocalization through an intricate approach which advances to consistency in bond strength [23].

3.2. Optical Analysis. The optical absorption measurements of the ZnO nanoparticles 300, 400, and 500°C are shown in Figure 3. The absorption spectrum of the nanoparticles synthesized at low temperature in Figure 3(a) (i) shows two absorption peaks located at 402 and 423 nm which can be ascribed to the presence of the ligand moiety in the surface of the nanoparticles. The spectrum also shows the band edge at 324 nm, whereas the spectra of the nanoparticles synthesized at higher temperatures (Figure 3(a) (ii)–(iii)) revealed band edges at 356 and 360 nm. All the absorption band edges were blue-shifted in comparison with the bulk ZnO [24].

The band-gap energies were calculated using Tauc's relationship [25]. The band-gap can be anticipated by Tauc's relationship between the optical absorption coefficient, α, the photon energy ($h\nu$), constant (A), and the direct band-gap energy (E_g) as shown in equation (1) below:

$$\alpha h\nu = A\left(h\nu - E_g\right)n, \tag{1}$$

where $n = 0.5$ for direct allowed transitions and $n = 2$ for indirect allowed transition. Plotting $(\alpha h\nu)^2$ versus photon energy ($h\nu$) and extrapolating the linear portion of the curve to absorption coefficient equal to zero can contribute the band-gap energy (Eg) values. Figure 3(b) displays the band-gap energies that were decreasing with the increase in decomposition temperature.

The emission spectra of ZnO nanoparticles (Figure 4) displayed emission maxima at 400, 412, and 429 nm which were red-shifted from the absorption band edges. The emission spectra of the nanoparticles prepared at higher temperatures (400 and 300°C) show the broad emission peaks which signify the polydispersity of the particles.

3.3. Structural Analysis. The XRD patterns of ZnO nanoparticles are represented in Figure 5. All the diffraction patterns of the synthesized nanoparticles were located around 2θ = 31.82°, 34.40°, 36.28°, 47.53°, 56.57°, 62.82°, 67.90°, and 68.88° that correspond to (100), (002), (101), (102), (110), (103), (112), and (201) planes which were indexed to hexagonal wurtzite structure of ZnO which matched with standard JCPDS data card No. 36–1451 with the cell constants of $a = b = 3.25$ Å and $c = 5.21$ Å which is matching with the previously reported results [26].

Figure 6 shows the TEM images of the synthesized ZnO nanoparticles that are spherical in shape. The synthesized particles were increasing in sizes and become agglomerated when the decomposition temperature was increased due to Ostwald ripening. The average particle sizes were found to be 2.56 ± 0.619, 6.36 ± 1.27, and 8.79 ± 2.43 nm for ZnO nanoparticles prepared at 300 (i), 400 (ii), and (iii) 500°C, respectively.

3.4. Adsorption Studies. Numerous factors such as pH, contact time, and initial metal ion concentration that affect the removal of Fe(II) ions from wastewater have been investigated. The solution was filtered after the adsorption processes and analyzed with flame atomic absorption spectrophotometry (AAS). The percentage removal of Fe(II) ions from wastewater was then calculated as reported previously [27] using the following formula equation (2):

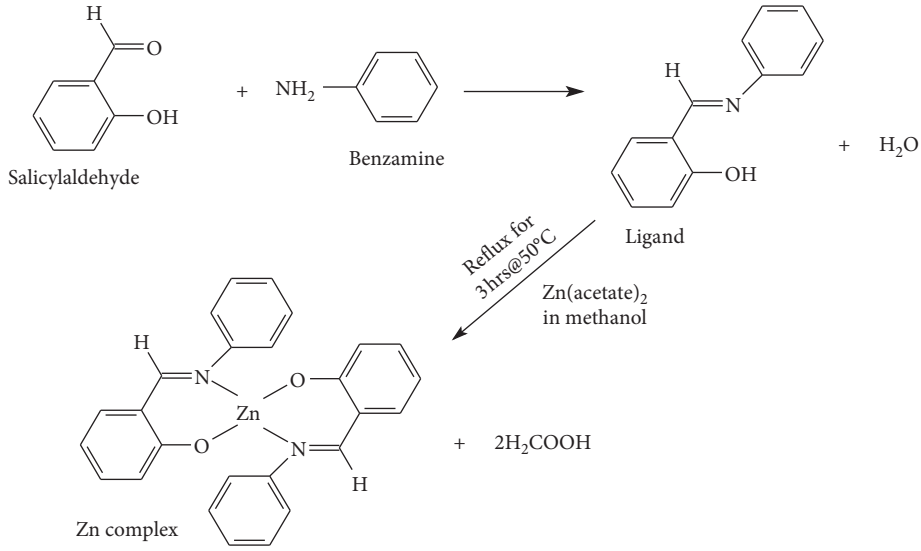

Scheme 1: Preparation of *bis*(N-benzyl-salicydenaminato)zinc (II) complex.

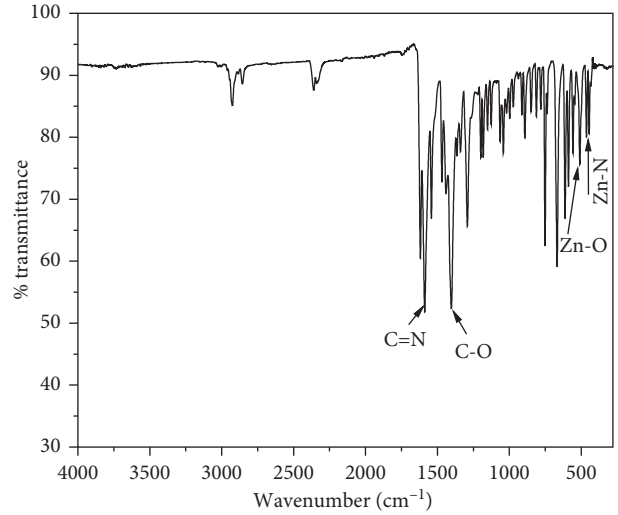

Figure 1: FTIR spectrum of *bis*(N-benzyl-salicydenaminato)zinc (II) complex.

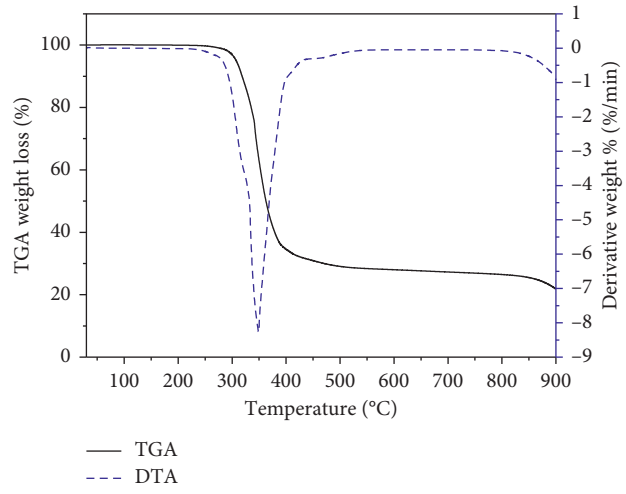

Figure 2: TGA/DTA curves of *bis*(N-benzyl-salicydenaminato)zinc (II) complex.

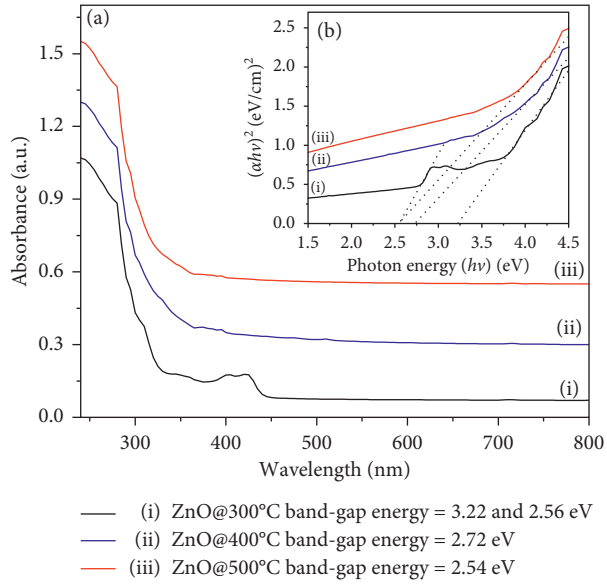

Figure 3: Absorption spectra (a) and Tauc plot (b) of the ZnO nanoparticles synthesized at 300 (i), 400 (ii), and 500°C (iii).

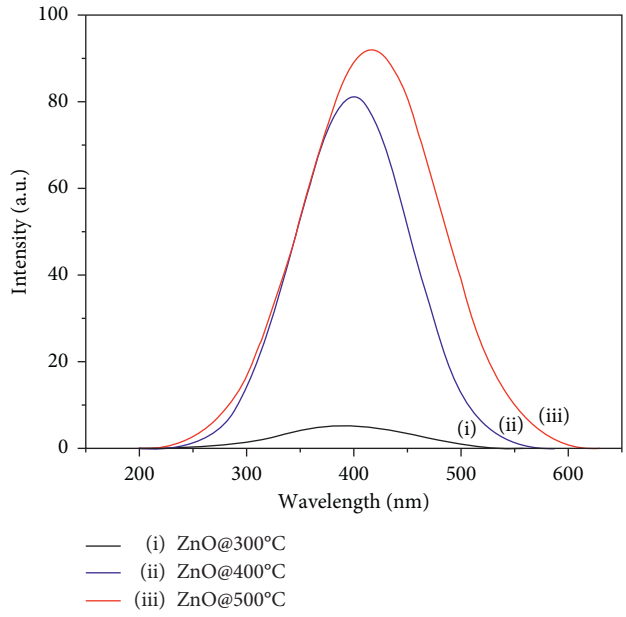

Figure 4: Emission spectra of ZnO nanoparticles synthesized at 300 (i), 400 (ii), and 500°C (iii).

$$\%\text{removal} = \frac{C_o - C_x}{C_o} \times 100\%, \quad (2)$$

where C_o (ppm) is the initial metal ion concentration and C_x (ppm) is the final metal ion concentration in the solution.

3.4.1. Effect of pH, Contact Time, and Initial Concentration. The solutions of chitosan and ZnO-chitosan nanocomposites were used as adsorbents to investigate the effect of pH of 50 ppm of Fe(II) solution (20 mL). The solution was stirred for 10 minutes and filtered. The maximum percentage removal of Fe(II) ion from the solution in Figure 7(a) was discovered to be about 62.99% for pure chitosan solution and 83.37% for ZnO-chitosan nanocomposites when the pH was elevated. The optimal pH was found to be 6.

To study the effect of contact time (Figure 7(b)), 50 ppm of the iron (II) solution (20.00 mL) was poured into different beakers. Each beaker was treated with 5 mL nanocomposites or chitosan and stirred at different times (10, 30, 60, 120, 240, and 480 min). The results showed that 120 minutes was the optimum contact time for both adsorbents which is similar to the reported results by Xaba et al. [28].

The effect of initial metal ion concentration of ZnO-chitosan and pure chitosan solutions on the percentage removal of Fe(II) ion is shown in Figure 7(c). The initial

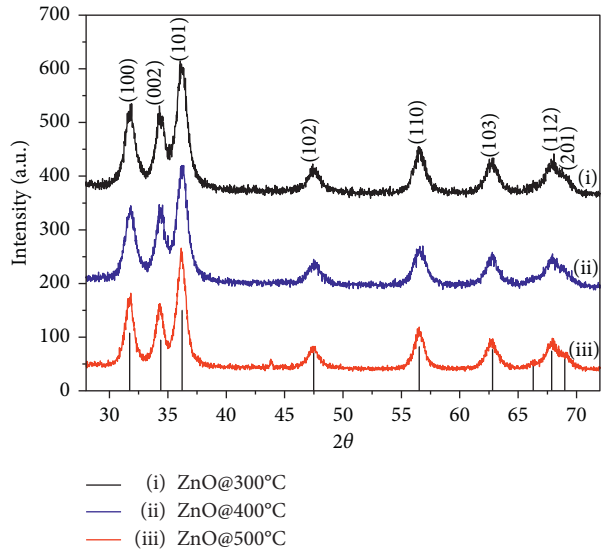

Figure 5: X-ray diffraction patterns of the ZnO nanoparticles synthesized at 300 (i), 400 (ii), and 500°C (iii).

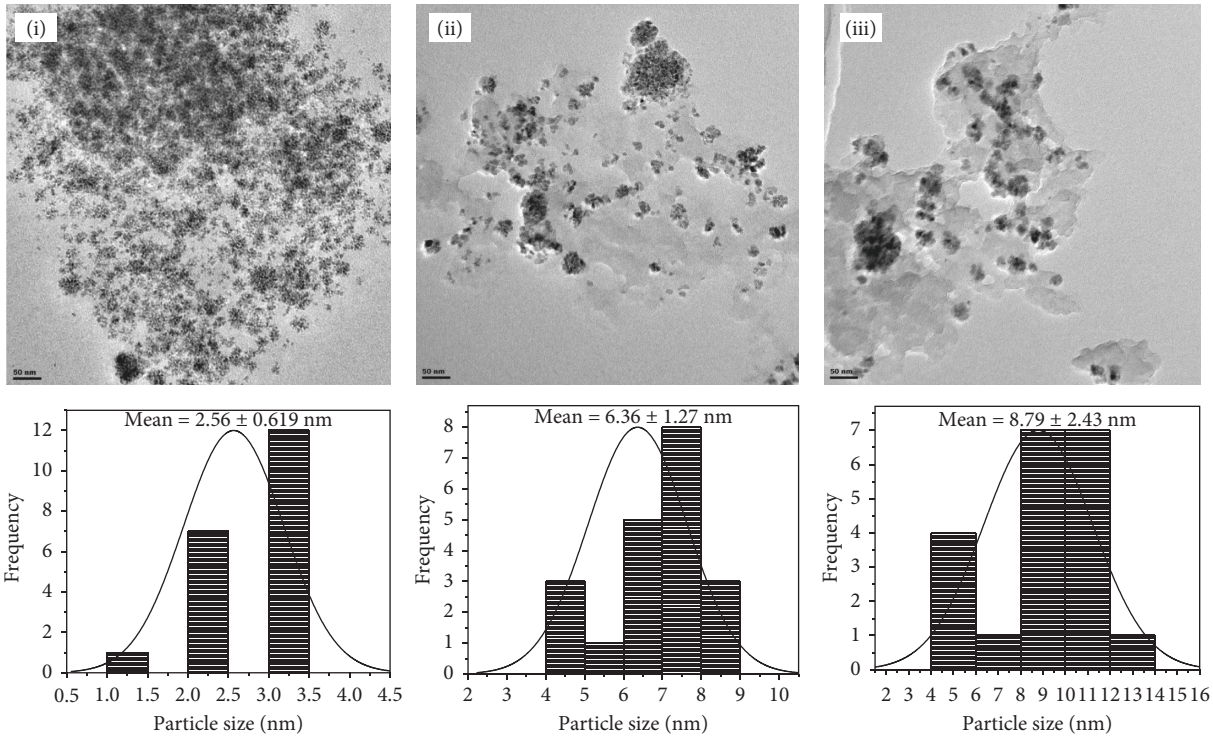

Figure 6: TEM images of ZnO nanoparticles synthesized at 300 (i), 400 (ii), and 500°C (iii).

concentration was varied from 50 to 200 mg/L. The results show that as the initial concentration is increased, the percentage removal decreases due to the volume gradient influence of the solution and adsorbent which is similar to the reported results [29].

4. Conclusion

The *bis*(N-benzyl-salicydenaminato)zinc (II) complex was prepared and characterized using spectroscopic and elemental analysis. The FTIR results showed the expected significant bands, and TGA displayed a single-stage decomposition which confirmed the purity of the complex. The ZnO nanoparticles were successfully synthesized through the thermal decomposition of the zinc precursor. The effect of various calcination temperatures was also studied. The optical properties revealed an increase in wavelength of the band edges and emission peaks when the decomposition temperature was elevated. The results also disclosed that the band-gap energy of the synthesized ZnO can be regulated by

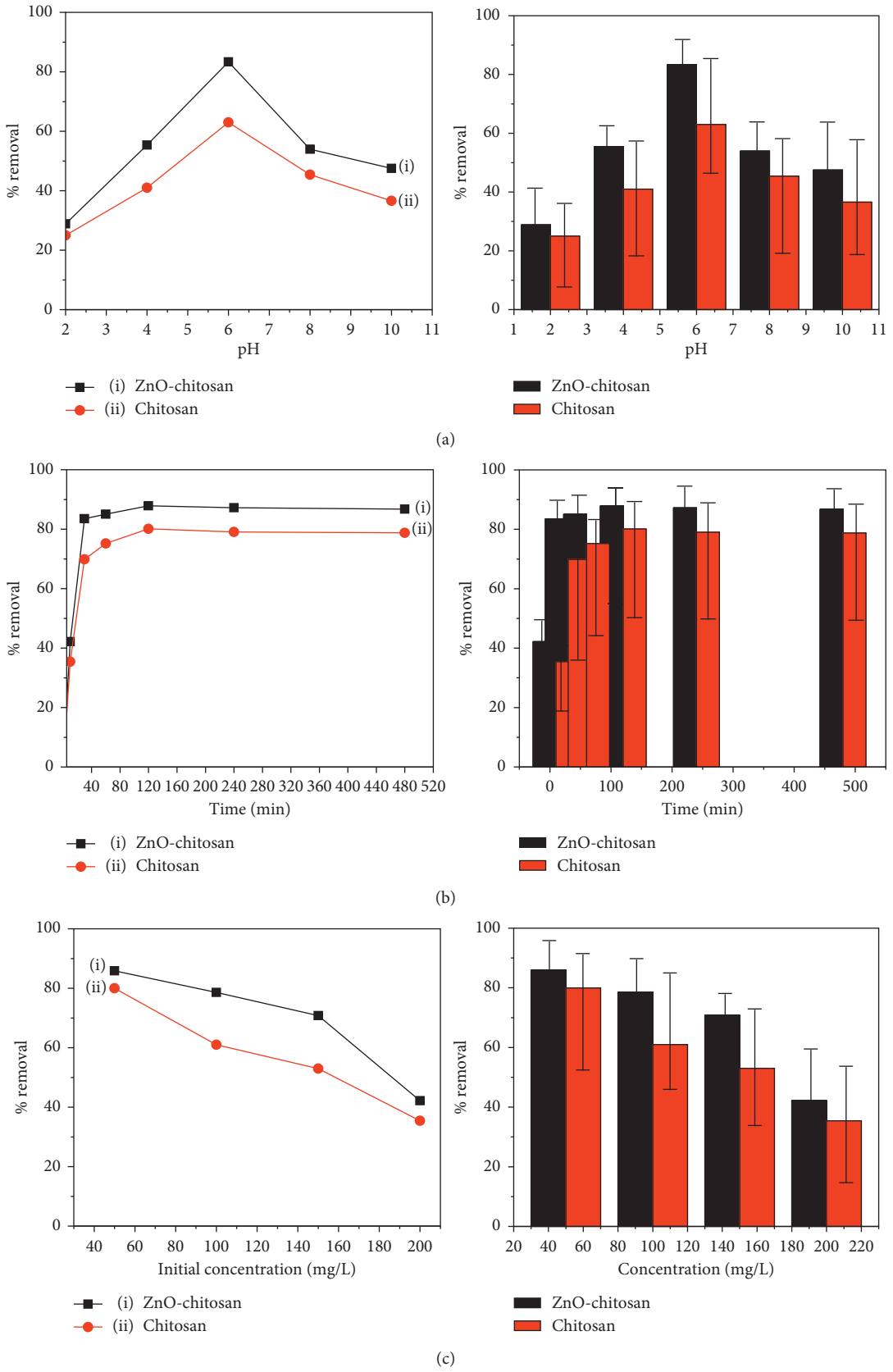

Figure 7: Effect of pH (a), contact time (b), and initial concentration (c) on adsorption of Fe(II) ion using ZnO-chitosan nanocomposites (i) and chitosan (ii) as adsorbents.

varying the growth temperature. The XRD patterns exhibited a hexagonal phase for all the synthesized particles. The TEM images showed that when the temperature was increased, the particles were increasing in sizes. The images also revealed the agglomerated particles at higher temperatures. ZnO-chitosan nanocomposite displayed the better percentage removal of Fe(II) ions compared to chitosan solution.

Data Availability

The data used to support the findings of this study are available from the corresponding author upon request.

Conflicts of Interest

The authors declare that there are no conflicts of interest regarding the publication of this article.

Acknowledgments

The authors would like to appreciate financial support from the Vaal University of Technology and National Research Foundation (NRF) (Thuthuka Grant Holder no. TTK170508230117).

References

[1] Q. Wang, J. Song, and M. Sui, "Characteristic of adsorption, desorption and oxidation of Cr (III) on birnessite," *Energy Procedia*, vol. 5, pp. 1104–1108, 2011.

[2] M. Immamuglu and O. Tekir, "Removal copper (II) and lead(II) ions from aqueous solutions by adsorption on activated carbon from a new precursor hazelnut husks," *Desalination*, vol. 228, no. 1–3, pp. 108–113, 2008.

[3] S. Vasudevan, J. Lakshmi, and G. Sozhan, "Studies on the removal of iron from drinking water by electrocoagulation-a clean process," *CLEAN-Soil, Air, Water*, vol. 37, no. 1, pp. 45–51, 2009.

[4] C. K. Ahn, Y. M. Kim, S. H. Woo, and J. M. Park, "Removal of cadmium using acid-treated activated carbon in the presence of nonionic and/or anionic surfactants," *Hydrometallurgy*, vol. 99, no. 3-4, pp. 209–213, 2009.

[5] W. C. Leung, M.-F. Wong, H. Chua, W. Lo, P. H. F. Yu, and C. K. Leung, "Removal and recovery of heavy metals by bacteria isolated from activated sludge treating industrial effluents and municipal wastewater," *Water Science and Technology*, vol. 41, no. 12, pp. 233–240, 2000.

[6] H. Mirzaei and M. Darroudi, "Zinc oxide nanoparticles: biological synthesis and biomedical applications," *Ceramics International*, vol. 43, no. 1, pp. 907–914, 2017.

[7] M. Rajalakshmi, S. Sohila, S. Ramya, R. Divakar, C. Ghosh, and S. Kalavathi, "Blue green and UV emitting ZnO nanoparticles synthesized through a non-aqueous route," *Optical Materials*, vol. 34, no. 8, pp. 1241–1245, 2012.

[8] Z. Deng, M. Chen, G. Gu, and L. Wu, "A facile method to fabricate ZnO hollow spheres and their photocatalytic property," *Journal of Physical Chemistry B*, vol. 112, no. 1, pp. 16–22, 2008.

[9] J. Zhang, D. Gao, G. Yang, Z. Zhu, J. Zhang, and Z. Shi, "Study on synthesis and optical properties of ZnO hierarchical nanostructures by hydrothermal method," *International Journal of Mechanical and Materials Engineering*, vol. 1, pp. 138–143, 2012.

[10] P.-J. Lu, S.-C. Huang, Y.-P. Chen, L.-C. Chiueh, and D. Y.-C. Shih, "Analysis of titanium dioxide and zinc oxide nanoparticles in cosmetics," *Journal of Food and Drug Analysis*, vol. 23, no. 3, pp. 587–594, 2015.

[11] P. K. Mishra, H. Mishra, A. Ekielski, S. Talegaonkar, and B. Vaidya, "Zinc oxide nanoparticles: a promising nanomaterial for biomedical applications," *Drug Discovery Today*, vol. 22, no. 12, pp. 1825–1834, 2017.

[12] L. Spaniel and M. A. Anderson, "Semiconductor clusters in the sol–gel process: quantized aggregation, gelation, and crystal growth in concentrated zinc oxide colloids," *Journal of American Chemical Society*, vol. 113, no. 8, pp. 2826–2833, 1991.

[13] A. Yadav, V. Prasad, A. A. Kathe et al., "Functional finishing in cotton fabrics using zinc oxide nanoparticles," *Bulletin of Materials Science*, vol. 29, no. 6, pp. 641–645, 2006.

[14] S. B. S. K. Pal and J. Dutta, "Nanostructured zinc oxide for water treatment," *Nanoscience and Nanotechnology-Asia*, vol. 2, no. 2, pp. 90–102, 2012.

[15] A. M. El Saeed, M. A. El-Fattah, and A. M. Azzam, "Synthesis of ZnO nanoparticles and studying its influence on the antimicrobial, anticorrosion and mechanical behavior of polyurethane composite for surface coating," *Dyes and Pigments*, vol. 121, pp. 282–289, 2015.

[16] S. Kumar, A. Thakur, V. S. Rangra, and S. Sharma, "Synthesis and use of low-band-gap ZnO nanoparticles for water treatment," *Arabian Journal for Science and Engineering*, vol. 41, no. 7, pp. 2393–2398, 2015.

[17] E. A. S. Dimapilis, C.-S. Hsu, R. M. O. Mendoza, and M.-C. Lu, "Zinc oxide nanoparticles for water disinfection," *Sustainable Environment Research*, vol. 28, no. 2, pp. 47–56, 2018.

[18] M. Thirumavalavan, K.-L. Huang, and J.-F. Lee, "Preparation and morphology studies of nano zinc oxide obtained using native and modified chitosans," *Materials*, vol. 6, no. 9, pp. 4198–4212, 2013.

[19] S. Vasudevan, J. Jayaraj, J. Lakshmi, and G. Sozhan, "Removal of iron from drinking water by electrocoagulation: adsorption and kinetics studies," *Korean Journal of Chemical Engineering*, vol. 26, no. 4, pp. 1058–1064, 2010.

[20] S. Vasudevan, "Effects of alternating current (AC) and direct current (DC) in electrocoagulation process for the removal of iron from water," *Canadian Journal of Chemical Engineering*, vol. 90, no. 5, pp. 1160–1169, 2011.

[21] S. Vasudevan and M. A. Oturan, "Electrochemistry: as cause and cure in water pollution-an overview," *Environmental chemistry letters*, vol. 12, no. 1, pp. 97–108, 2013.

[22] T. Akitsu and Y. Einaga, "Synthesis and crystal structures of the flexible Schiff base complex bis(N-1,2-diphenylethyl-salicydenaminato-κ2N,O)copper(II) (methanol): a rare case of solvent-induced distortion," *Polyhedron*, vol. 25, no. 5, pp. 1089–1095, 2006.

[23] S. S. Swathy, R. Selwin Joseyphus, V. P. Nisha, N. Subhadrambika, and K. Mohanan, "Synthesis, spectroscopic investigation and antimicrobial activities of some transition metal complexes of a [(2-hydroxyacetophenone)-3-isatin]-bishydrazone," *Arabian Journal of Chemistry*, vol. 9, no. 2, pp. 1847–1857, 2016.

[24] Z. L. Wang, "Zinc oxide nanostructures: growth, properties and applications," *Journal of Physics: Condensed Matter*, vol. 16, no. 25, pp. 829–858, 2004.

[25] J. Tauc, R. Grigorovici, and A. Vancu, "Optical properties and electronic structure of amorphous germanium," *Physica Status Solidi (b)*, vol. 15, no. 2, pp. 627–637, 1966.

[26] Z.-P. Sun, L. Liu, L. Zhang, and D.-Z. Jia, "Rapid synthesis of ZnO nano-rods by one-step, room-temperature, solid-state reaction and their gas-sensing properties," *Nanotechnology*, vol. 17, no. 9, pp. 2266–2270, 2006.

[27] T. Xaba, M. J. Moloto, O. Nchoe, Z. Nate, and N. Moloto, "Synthesis of silver sulfide nanoparticles through homogeneous precipitation route and the preparation of the Ag_2S-chitosan nanocomposites for the removal of iron(II) ion from wastewater," *Chalcogenide Letters*, vol. 14, no. 8, pp. 337–346, 2017.

[28] T. Xaba, J. Magagula, and O. B. Nchoe, ""Green" synthesis of Cu 2 S nanoparticles from (Z)-1-methyl-2-(pyrrolidin-2-ylidene)thiourea ligand for the preparation of Cu 2 S-chitosan nanocomposites for the removal of Cr(VI) ion from wastewater," *Materials Letters*, vol. 229, pp. 331–335, 2018.

[29] A. G. Hadi, "Removal of Fe (II) and Zn (II) ions from aqueous solutions by synthesized chitosan," *International Journal of Chem-Tech Research*, vol. 9, no. 4, pp. 343–349, 2016.